

## Metal–Polypyridyl Catalysts for Electro- and Photochemical Reduction of Water to Hydrogen

Published as part of the Accounts of Chemical Research special issue “Earth Abundant Metals in Homogeneous Catalysis”.

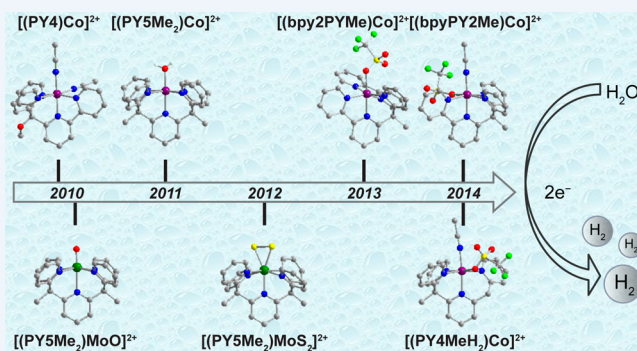
David Z. Zee,<sup>†,‡,∇</sup> Teera Chantarojsiri,<sup>†,∇</sup> Jeffrey R. Long,<sup>\*,†,⊥,‡,#</sup> and Christopher J. Chang<sup>\*,†,‡,§,||</sup>

Departments of <sup>†</sup>Chemistry and <sup>‡</sup>Molecular and Cell Biology and the <sup>§</sup>Howard Hughes Medical Institute, University of California, Berkeley, Berkeley, California 94720, United States

<sup>||</sup>Chemical Sciences Division and <sup>⊥</sup>Materials Sciences Division and the <sup>#</sup>Joint Center for Artificial Photosynthesis, Lawrence Berkeley National Laboratory, Berkeley, California 94720, United States

**CONSPECTUS:** Climate change, rising global energy demand, and energy security concerns motivate research into alternative, sustainable energy sources. In principle, solar energy can meet the world’s energy needs, but the intermittent nature of solar illumination means that it is temporally and spatially separated from its consumption. Developing systems that promote solar-to-fuel conversion, such as via reduction of protons to hydrogen, could bridge this production–consumption gap, but this effort requires invention of catalysts that are cheap, robust, and efficient and that use earth-abundant elements. In this context, catalysts that utilize water as both an earth-abundant, environmentally benign substrate and a solvent for proton reduction are highly desirable. This Account summarizes

our studies of molecular metal–polypyridyl catalysts for electrochemical and photochemical reduction of protons to hydrogen. Inspired by concept transfer from biological and materials catalysts, these scaffolds are remarkably resistant to decomposition in water, with fast and selective electrocatalytic and photocatalytic conversions that are sustainable for several days. Their modular nature offers a broad range of opportunities for tuning reactivity by molecular design, including altering ancillary ligand electronics, denticity, and/or incorporating redox-active elements. Our first-generation complex,  $[(PY4)Co(CH_3CN)_2]^{2+}$ , catalyzes the reduction of protons from a strong organic acid to hydrogen in 50% water. Subsequent investigations with the pentapyridyl ligand PY5Me<sub>2</sub>, furnished molybdenum and cobalt complexes capable of catalyzing the reduction of water in fully aqueous electrolyte with 100% Faradaic efficiency. Of particular note, the complex  $[(PY5Me_2)MoO]^{2+}$  possesses extremely high activity and durability in neutral water, with turnover frequencies at least 8500 mol of H<sub>2</sub> per mole of catalyst per hour and turnover numbers over 600 000 mol of H<sub>2</sub> per mole of catalyst over 3 days at an overpotential of 1.0 V, without apparent loss in activity. Replacing the oxo moiety with a disulfide affords  $[(PY5Me_2)MoS_2]^{2+}$ , which bears a molecular MoS<sub>2</sub> triangle that structurally and functionally mimics bulk molybdenum disulfide, improving the catalytic activity for water reduction. In water buffered to pH 3, catalysis by  $[(PY5Me_2)MoS_2]^{2+}$  onsets at 400 mV of overpotential, whereas  $[(PY5Me_2)MoO]^{2+}$  requires an additional 300 mV of driving force to operate at the same current density. Metalation of the PY5Me<sub>2</sub> ligand with an appropriate Co(II) source also furnishes electrocatalysts that are active in water. Importantly, the onset of catalysis by the  $[(PY5Me_2)Co(H_2O)]^{2+}$  series is anodically shifted by introducing electron-withdrawing functional groups on the ligand. With the  $[(bpy2PYMe)Co(CF_3SO_3)]^{1+}$  system, we showed that introducing a redox-active moiety can facilitate the electro- and photochemical reduction of protons from weak acids such as acetic acid or water. Using a high-throughput photochemical reactor, we examined the structure–reactivity relationship of a series of cobalt(II) complexes. Taken together, these findings set the stage for the broader application of polypyridyl systems to catalysis under environmentally benign aqueous conditions.



### ■ INTRODUCTION

Increasing global demand for energy and concerns over anthropogenic climate change drive the search for sustainable, alternative energy sources. Solar energy is a preeminent candidate, as it achieves the scale needed to meet the demand, but it suffers from critical problems in energy storage and transport.<sup>1</sup> One attractive solution to this problem is solar-to-fuel conversion, where energy is stored by converting energy-poor molecules into energy-rich ones. In particular, hydrogen is an

appealing carbon-neutral fuel, as both its feedstock and combustion product are water.<sup>2</sup> Platinum can catalyze the reduction of water to hydrogen at fast rates near thermodynamic equilibrium, but its low abundance and high cost prohibit its widespread use.<sup>3</sup> As such, it is attractive to develop inexpensive, earth-abundant hydrogen-evolution catalysts that can, when

Received: February 17, 2015

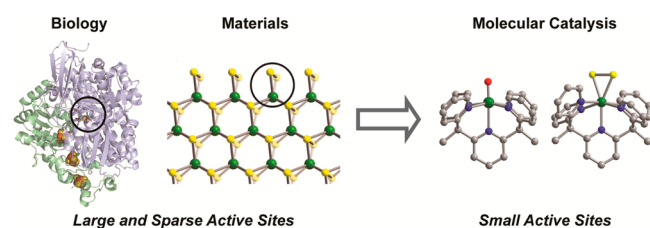


**Figure 1.** Hydrogenase enzymes (far left) and MoS<sub>2</sub> (molybdenite, second from left) are proton reduction catalysts from biology and materials, respectively. Black circles delineate the small and sparse active sites among the large, overall structures: the [NiFe] cofactor of [NiFe]-hydrogenase enzymes (molecular weight ~60 000 kDa) and the disulfide-terminated (1 0 -1 0) edge of MoS<sub>2</sub>. Molecular catalysts (right) can capture the functional essence of these biological and materials systems in a compact and tunable active site.

interfaced with electrodes or photoelectrodes, convert solar energy into chemical energy in a sustainable manner.<sup>4</sup>

In this context, biology and materials provide unifying concepts to drive the development of new solar-fuel chemistry. Within the framework of hydrogen production, hydrogenase enzymes can convert protons and electrons to hydrogen utilizing only iron and/or nickel in their active sites with high speed and efficiency on a per molecule basis.<sup>5,6</sup> However, the activity of enzymes on a per volume basis is limited by size constraints, as most of the protein structure is devoted to its biological regulation for cellular function while critical catalytic reactions occur at relatively small active sites within these larger scaffolds (Figure 1). A similar situation is observed in

heterogeneous materials, where catalytically active sites are often restricted to minor edges or faces and the bulk of the material is inert and provides but a scaffold for stability purposes. With these principles in mind, molecular catalysts can retain the small, functional units of their biological or materials counterparts but can achieve higher volumetric activities by discarding the superfluous regulatory or stabilizing scaffolds. Indeed, molecular proton reduction catalysis is a vibrant area of research and has been the subject of numerous excellent and comprehensive reviews.<sup>7–15</sup> A key challenge is achieving efficient and sustainable catalysis in water, and we focus this Account on strategic efforts from our laboratories to meet this goal by employing metal–polypyridyl complexes.

## ■ POLYPYRIDYL LIGANDS FOR CATALYSIS IN WATER

An important goal of proton reduction catalysis is to use water as both substrate and solvent, as water is the most abundant source of protons and offers the benefit of maintaining high substrate concentrations without organic waste produced during fuel generation or combustion. In this regard, many elegant examples of molecular proton reduction catalysts have been reported, but aqueous compatibility remains a challenge, as many molecular catalysts lack solubility in water, whereas others are irreversibly decomposed by water and cannot be funneled back into the catalytic pathway. Our research program has centered on multidentate polypyridine ligands to address these issues. First, the use of a neutral polypyridyl scaffold coordinated to a metal ion gives a charged complex, which, combined with an appropriate charge-balancing anion, provides aqueous solubility. Moreover, being aromatic and possessing strong bonds, pyridine ligands are

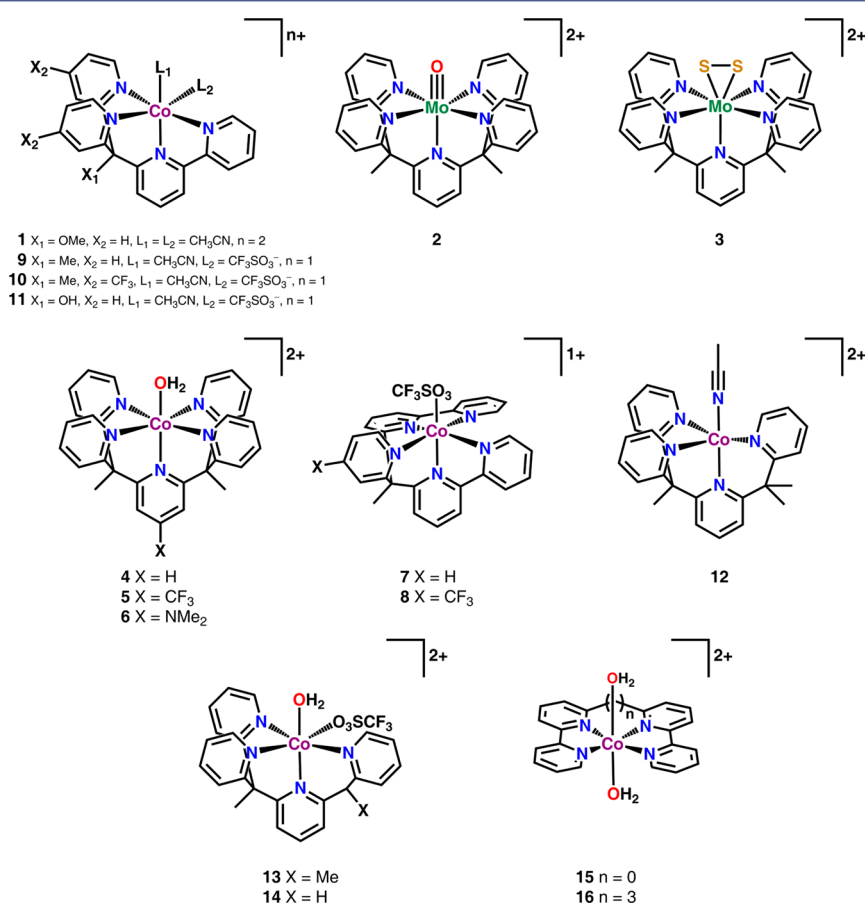


**Figure 2.** Molecular metal–polypyridyl H<sub>2</sub> evolution catalysts from our laboratories.

Table 1. CPE Data of Hydrogen-Producing Catalysts

	applied potential ( $\eta^a$ )	Faradaic efficiency (%)	TON (reaction time) (mol H <sub>2</sub> (mol cat) <sup>-1</sup> )	TOF (mol H <sub>2</sub> (mol cat h) <sup>-1</sup> )	electrode <sup>b</sup>	electrolyte	ref
1	-1.40 V vs Fc <sup>+0</sup> (0.62 V)	99	— <sup>c</sup>	40 <sup>d</sup>	GC	65 mM TFA <sup>e</sup> in CH <sub>3</sub> CN <sup>f</sup>	16
2	-1.40 V vs SHE (0.99 V)	100	610 000 (72 h)	8500 <sup>g</sup>	Hg	3.0 M pH 7 phosphate in H <sub>2</sub> O	26
2	-2.24 V vs Fc <sup>+0</sup> (0.90 V)	99	3.7 (1 h)	3.7 <sup>g</sup>	GC	170 equiv AcOH <sup>h</sup> in CH <sub>3</sub> CN <sup>f</sup>	27
3	-0.96 V vs SHE (0.78 V)	100	19 000 000 (23 h) <sup>i</sup>	830 000 <sup>ij</sup>	Hg	3.0 M pH 3 acetate in H <sub>2</sub> O	35
3	-1.73 V vs Fc <sup>+0</sup> (0.39 V)	100	5.7 (2.75 h)	2.1 <sup>g</sup>	GC	160 equiv AcOH <sup>h</sup> in CH <sub>3</sub> CN <sup>f</sup>	35
4	-1.30 V vs SHE (0.89 V)	100	55 000 (60 h)	920 <sup>g</sup>	Hg	2.0 M pH 7 phosphate in H <sub>2</sub> O	36
5	-0.96 V vs SHE (0.55 V)	95	— <sup>c</sup>	— <sup>c</sup>	GC	0.1 M pH 7 phosphate in H <sub>2</sub> O	41
7	-1.80 V vs Fc <sup>+0</sup> (0.46 V)	90	— <sup>c</sup>	— <sup>c</sup>	GC	AcOH <sup>h</sup> in CH <sub>3</sub> CN <sup>f</sup>	64

<sup>a</sup> $\eta$  = overpotential = applied potential - (0.059 V × pH) in water.  $\eta$  = applied potential - [( $E^\circ_{\text{H}^+/\text{H}_2}$ ) - (0.059 V × pH)] for nonaqueous systems.<sup>71</sup>  
<sup>b</sup>GC, glassy carbon <sup>c</sup>—, no published data available. <sup>d</sup>Estimated from CV data. <sup>e</sup> $E^\circ = -0.78$  V vs Fc<sup>+0</sup>. <sup>f</sup>With 0.1 M NBu<sub>4</sub>PF<sub>6</sub> as supporting electrolyte. <sup>g</sup>These numbers are estimated from the CPE data under the assumption that all catalyst molecules in solution participate in the reaction at any given time. Thus, they represent a *lower bound* of the true TOF. <sup>h</sup> $E^\circ = -1.34$  V vs Fc<sup>+0</sup>. <sup>i</sup>Calculated based on the estimated surface coverage of the catalyst on the Hg pool. <sup>j</sup>In an optimized medium, the TOF reaches 480 mol H<sub>2</sub> per mole catalyst per second.<sup>35</sup>

resistant to hydrolysis. Finally, we reasoned that the strong  $\sigma$ -donor capabilities of pyridines coupled with their ability to participate in metal-to-ligand  $\pi$  back-bonding should stabilize reduced metal species. Figure 2 summarizes water-compatible polypyridyl scaffolds that we have successfully applied in the catalytic reduction of protons to hydrogen.

### ■ A WATER-COMPATIBLE TETRAPYRIDYL-COBALT CATALYST

Our initial foray into electrocatalytic proton reduction centered on the cobalt(II) complex [(PY4)Co(CH<sub>3</sub>CN)<sub>2</sub>]<sup>2+</sup> (**1**, Figure 2).<sup>16</sup> The cyclic voltammogram (CV) of **1** in acetonitrile displays a reversible Co(II)/(I) redox couple at modest reduction potentials. Addition of trifluoroacetic acid (TFA) triggered proton reduction catalysis, with ~99% Faradaic yield (Table 1). Importantly, we found that electrocatalytic reduction of TFA by **1** was observed even when the water content in the electrolyte solution was increased to 50%, although the complex was insoluble at higher water levels (Figure 3). Nevertheless, the results established the viability of our strategy.

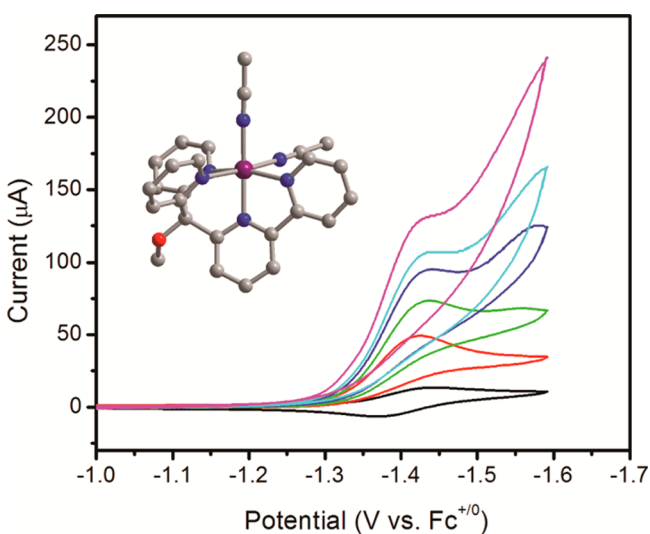


**Figure 3.** Cyclic voltammogram of **1** in a 1:1 water/CH<sub>3</sub>CN (v/v) mixture (black), with a glassy carbon working electrode. The Co(II/I) couple occurs ca. -1.4 V versus the ferrocenium/ferrocene couple (Fc<sup>+0</sup>). Increasing concentrations of TFA give corresponding rises of catalytic current (red, green, blue, cyan, and purple). The inset shows the crystal structure of **1**;  $R_1$  ( $wR_2$ ) = 5.20% (13.3%).

### ■ ELECTROCATALYTIC PROTON REDUCTION IN NEUTRAL WATER USING [(PY5Me<sub>2</sub>)MoO]<sup>2+</sup>

Concurrently, longstanding efforts in molecular magnetism led us to explore polypyridyl capping ligands to prepare coordination clusters. In particular, we became interested in the PYS ligand investigated by Stack and co-workers for bioinorganic model chemistry,<sup>17–19</sup> but we found its preparation to be synthetically challenging. As such, we developed a convenient, multigram-scale preparation for the related ligand, PY5Me<sub>2</sub>,<sup>20</sup> which enabled us to pursue parallel investigations in both molecular magnetism and reactivity.

Inspired by elegant water activation studies in the organometallic literature,<sup>21–25</sup> particularly the work of Yoon and Tyler<sup>23</sup> on MCp<sub>2</sub> fragments, we focused on low-valent molybdenum chemistry supported by PY5Me<sub>2</sub>. We reasoned that substituting the neutral PY5Me<sub>2</sub> for the anionic cyclopentadienyls would leave at least one open coordination site available for chemistry and shift reductions to more positive potentials, enabling reactivity nearer the thermodynamic potential for water reduction. Indeed, the Mo(II) complex [(PY5Me<sub>2</sub>)Mo(CF<sub>3</sub>SO<sub>3</sub>)]<sup>1+</sup> reacts with water to form the molybdenum(IV)-oxo ion [(PY5Me<sub>2</sub>)MoO]<sup>2+</sup> (**2**, Figure 2), with concomitant release of H<sub>2</sub>.<sup>26</sup> This quantitative stoichiometric reactivity encouraged us to test **2** as an electrocatalyst, and we were delighted to observe that it is capable of reducing acetic acid to hydrogen in acetonitrile at 100% Faradaic efficiency (Figure 4a, Table 1).<sup>27</sup> Cyclic and rotating disk voltammetry experiments unambiguously establish the active catalyst to be molecular in nature. Complex **2** proved to be sufficiently soluble and active in water, displaying two reduction events preceding a sharp rise in current corresponding to catalysis. Controlled-potential electrolyses (CPE) of **2** at -1.40 V versus the standard hydrogen electrode (SHE) showcase its activity and durability in water, with turnover frequencies (TOF) of at least 8500 mol of H<sub>2</sub> per mole of catalyst per hour, turnover numbers (TON) over 600 000 mol of H<sub>2</sub> per mole of catalyst after 72 h without loss of activity, and 100% Faradaic efficiency (Figure 4d, Table 1). Computational investigations suggest that in aqueous solution the first two reductions are proton-coupled and that those electrons are placed into orbitals antibonding in character with respect to the Mo–O bond to make the oxo moiety more nucleophilic and basic.<sup>28</sup> A third electron yields a Mo(I) center that cleaves the H–OH bond of the ligated water to form a seven-coordinate Mo(III) complex,



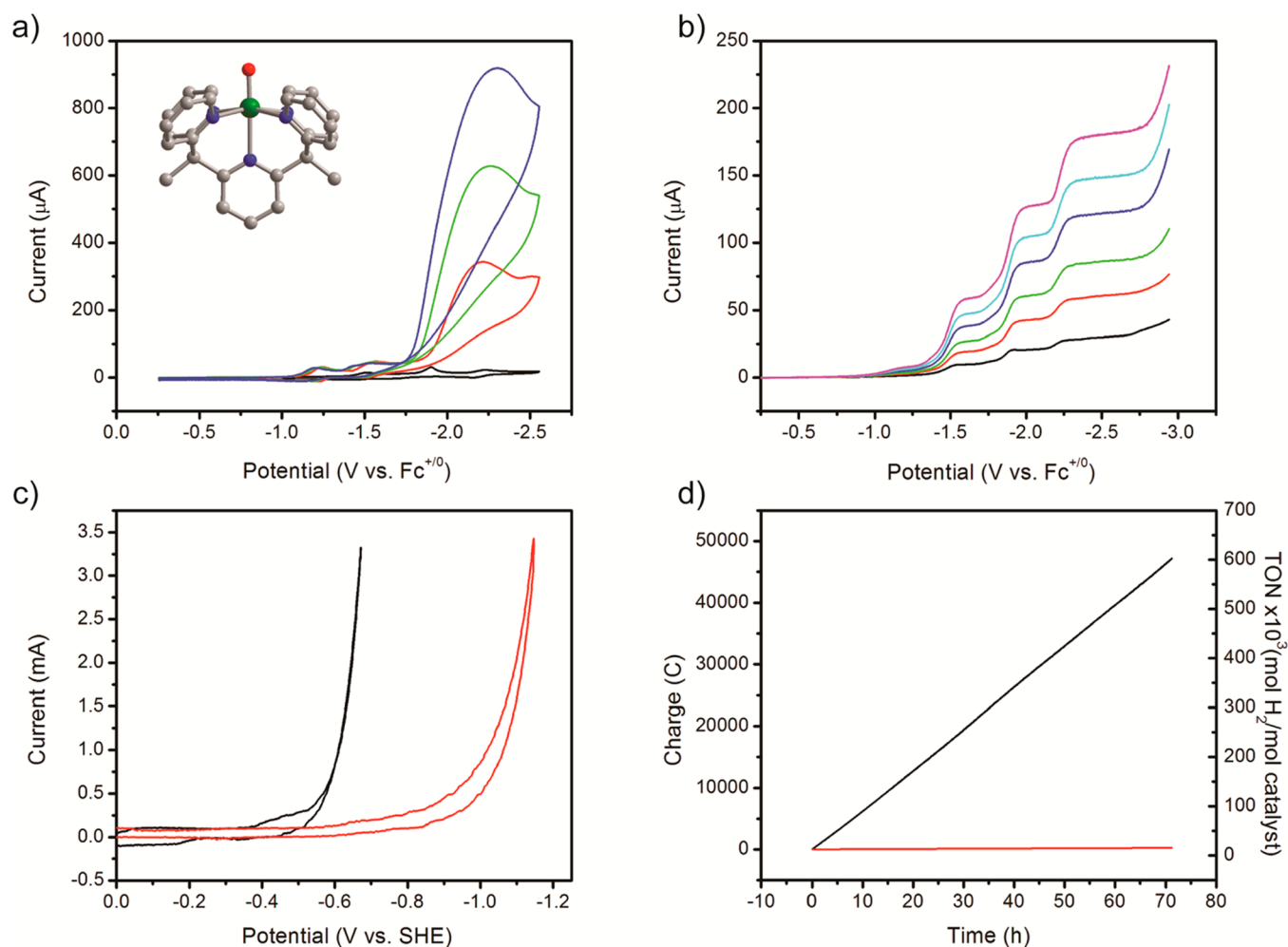


**Figure 4.** (a) CV of 2 in CH<sub>3</sub>CN at a glassy carbon electrode (black). Addition of acetic acid causes current enhancement at the third reduction, with plateaus occurring at ca. -2.25 V vs Fc<sup>+0</sup>. The inset shows the crystal structure of 2;  $R_1$  ( $wR_2$ ) = 3.64% (9.82%). (b) Rotating disk electrode voltammograms (100–3600 rpm) of 2 in CH<sub>3</sub>CN (glassy carbon). Traces show three distinct plateaus, indicating three reduction processes. (c) CV in a 0.6 M aqueous phosphate buffered to pH 7 at a Hg pool electrode in the absence (red) and presence of 2 (black). (d) CPE at -1.40 V vs SHE in the absence (red) and presence of 2 (2 μM, black) in 3.0 M phosphate buffered to pH 7. Complex 2 remains catalytically active after 72 h of electrolysis.

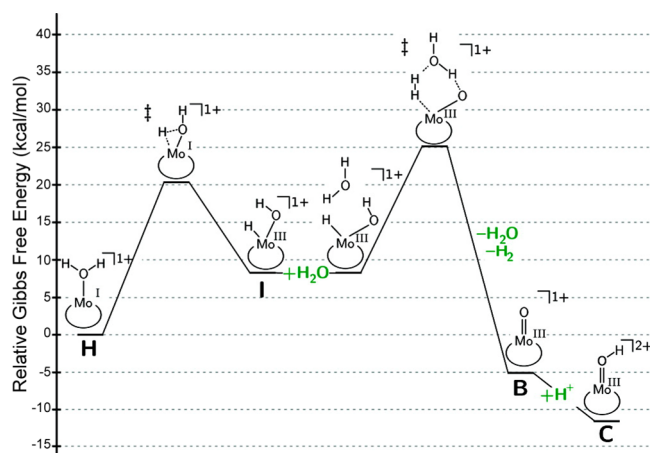


**Figure 5.** Gibbs free energy diagram for the liberation of H<sub>2</sub> from H, which is formed by the reduction of 2.

$[(\text{PYSMe}_2)\text{Mo}(\text{H})(\text{OH})]^{1+}$  (Figure 5). Finally, the catalyst was found to be highly active in unpurified seawater, suggesting that the PYSMe<sub>2</sub> ligand not only provides a catalytically active

molybdenum site but also prevents catalyst poisoning by adventitious impurities.

#### ■ $[(\text{PYSMe}_2)\text{MoS}_2]^{2+}$ AS A FUNCTIONAL MOLECULAR MIMIC OF MOLYBDENUM DISULFIDE

While investigating 2 for water reduction, we recognized growing efforts in using nanoparticulate and amorphous MoS<sub>2</sub> for this same purpose,<sup>29–34</sup> where catalysis is postulated to occur at MoS<sub>2</sub> triangular edges.<sup>29,30</sup> These observations prompted us to prepare the Mo(IV)–disulfide  $[(\text{PYSMe}_2)\text{MoS}_2]^{2+}$  (3, Figure 2) with a molecular MoS<sub>2</sub> triangle that not only structurally resembles the active edge sites of MoS<sub>2</sub> but also functionally supports catalytic activity for reduction of protons to hydrogen in water.<sup>35</sup> The CV of 3 in acetonitrile displays a set of well-defined and reversible reduction events at potentials more positive than those of 2, presaging that stabilization of the reduced states by the S<sub>2</sub><sup>2-</sup> moiety could result in a catalyst with lower overpotentials. Indeed, catalysis by 3 in acetonitrile or acidic water initiates at 400 mV of overpotential, whereas 2 requires an additional 300 mV of driving force to operate at similar current densities (Figure 6, Table 1). This redox tuning emphasizes the molecular nature of 3, which is additionally

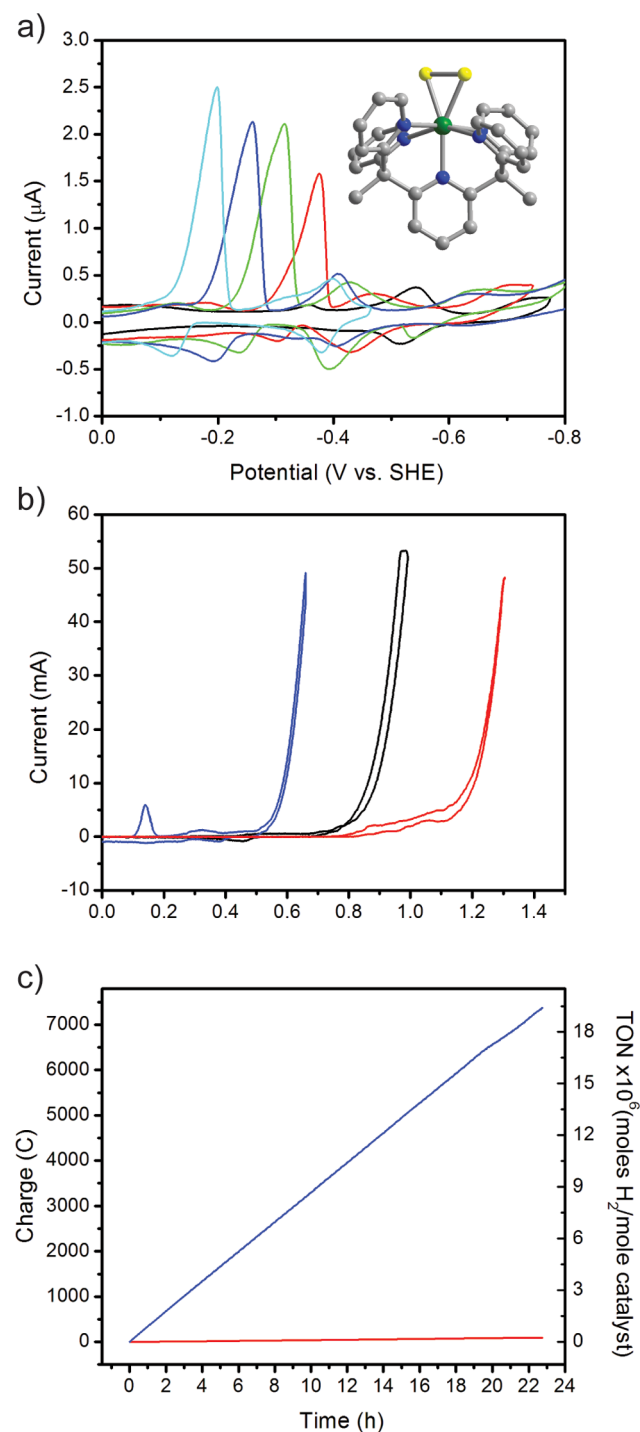


**Figure 6.** (a) CVs of **3** in 0.05 M phosphate buffered to pH ranging from 3 to 7. The first reductive wave shifts by ca. 60 mV per unit change in pH, suggesting that the reduction is proton-coupled. Inset shows the crystal structure of **3**;  $R_1$  ( $wR_2$ ) = 2.85% (6.08%). (b) CVs of 1 M acetate buffer at pH 3 at a mercury pool electrode (red) with **2** (130  $\mu$ M, black) and **3** (130  $\mu$ M, blue). (c) CPE of **3** (66  $\mu$ M) in 3 M aqueous acetate buffer (blue) versus the buffer alone (red) at  $-0.96$  V vs SHE ( $\eta = 0.78$  V).

confirmed by complementary electrochemical and spectroscopic experiments that show no evidence of Mo deposits. The catalyst also retains activity for at least 1 day with 100% Faradaic efficiency, and its sustained activity in untreated seawater again highlights the ability of the PYSMe<sub>2</sub> ligand to

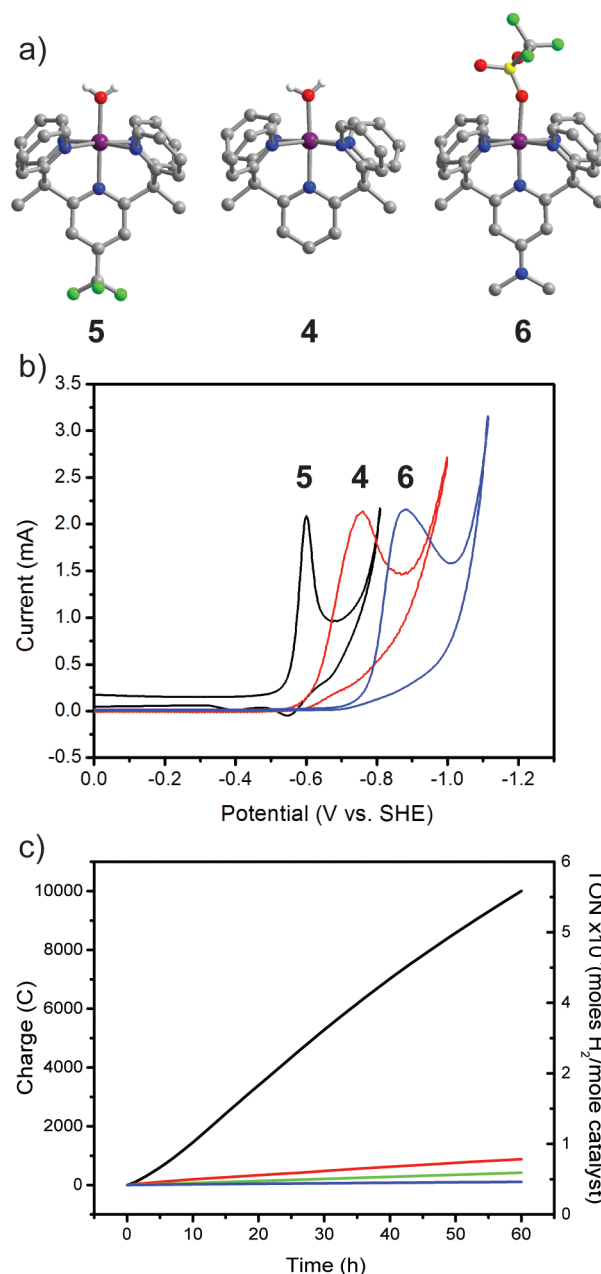


**Figure 7.** (a) Crystal structures of **4**, **5**, and **6**;  $R_1$  ( $wR_2$ ) = 3.04% (8.19%), 2.62% (6.67%), and 6.11% (18.9%), respectively. (b) Normalized CVs of **4** (red), **5** (black), and **6** (blue) in 1 M phosphate buffer at pH 7 at a Hg pool electrode. (c) CPE at  $-1.30$  V vs SHE of **4** (black), [(PYSMe<sub>2</sub>)Zn(H<sub>2</sub>O)]<sup>2+</sup> (green), PYSMe<sub>2</sub> ligand (red), and without additives (blue). Control experiments show that the ligand or metal alone or an isostructural PYSMe<sub>2</sub> complex with Zn(II) are inactive for catalysis. Only the CoPYSMe<sub>2</sub> unit shows competent reactivity. All electrolyses were performed in 2 M phosphate buffer at pH 7.

furnish robust transition metal catalysts in aqueous media. In a broader sense, this work establishes a path toward functional molecular mimics of heterogeneous catalysts, in analogy to the use of coordination complexes as models for enzyme active sites.

### ■ [(PYSMe<sub>2</sub>)Co(H<sub>2</sub>O)]<sup>2+</sup> AS A TUNABLE PLATFORM FOR WATER REDUCTION IN NEUTRAL WATER

Given the structural similarities between PYS and PYSMe<sub>2</sub>, as well as the established use of the former as a ligand for first-row

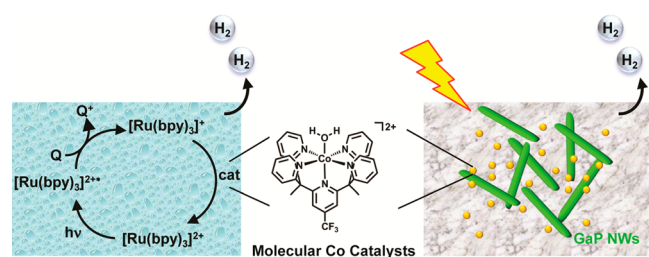


**Figure 8.** Photochemical generation of H<sub>2</sub> by **5** photosensitized with either [Ru(bpy)<sub>3</sub>]<sup>2+</sup> (left) or GaP nanowires (right), with ascorbate as a sacrificial reductant.

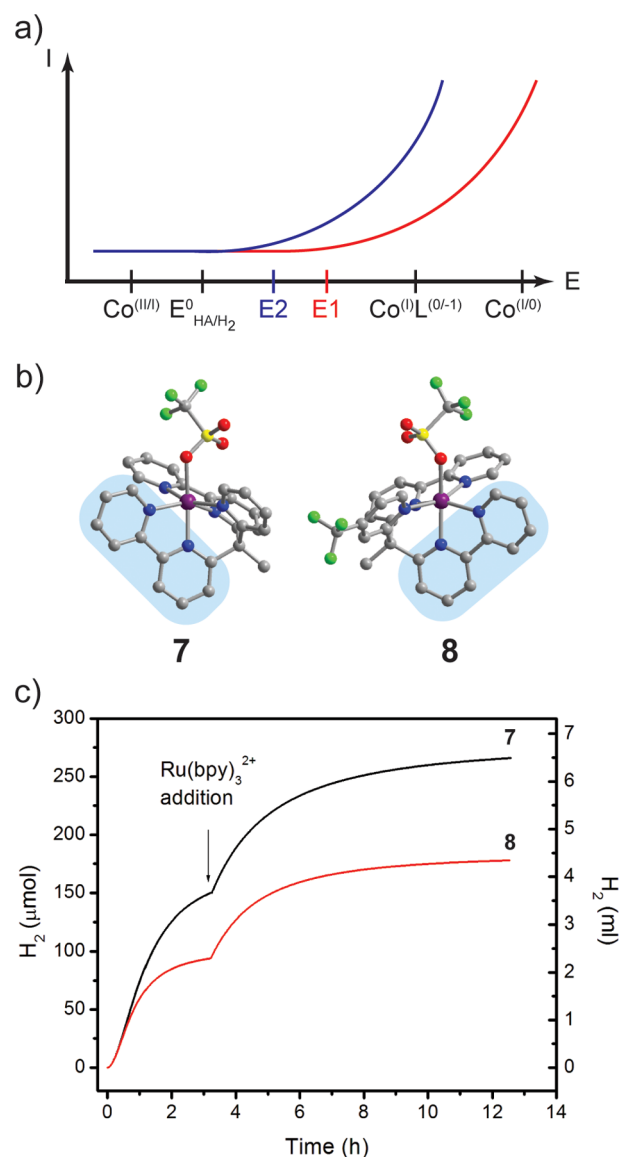


**Figure 9.** (a) To reduce a weak acid such as water, catalysis may involve a Co(II/0) process, with a driving force of E1 (red). Introduction of a ligand-based redox state gives a new driving force, E2, that can afford catalysis at less extreme potentials (blue). (b) Crystal structures of **7** and **8**;  $R_1$  ( $wR_2$ ) = 3.61% (9.25%) and 3.32% (7.83%), respectively. Blue areas highlight one of the redox-active bpy moieties. (c) Photocatalytic H<sub>2</sub> evolution in water by **7** and **8**. Once catalysis levels off, addition of [Ru(bpy)<sub>3</sub>]<sup>2+</sup> regenerates activity.

transition metals, we reasoned that the PYSMe<sub>2</sub> ligand could support first-row transition metal water reduction catalysts with

the reactivity, durability, and solubility necessary to function in aqueous media. Indeed, CVs collected in water with [(PYSMe<sub>2</sub>)Co(H<sub>2</sub>O)]<sup>2+</sup> (**4**, Figure 2)<sup>36</sup> show an irreversible reduction followed by hydrogen evolution catalysis (Figure 7b). Like its molybdenum predecessors, electrolysis with **4** generates H<sub>2</sub> with 100% Faradaic efficiency for at least 60 h (Figure 7c, Table 1), suggesting that the PYSMe<sub>2</sub> ligand helps prevent decomposition via nonproductive pathways.

Although **4** operates at a fairly high overpotential, the most salient feature of this system is the ability to tune potentials in a rational molecular manner. Introduction of an electron-withdrawing trifluoromethyl substituent at the 4-position of the central pyridine affords the electronically deficient complex **5** (Figure 2) and anodically shifts the initial one-electron reduction and subsequent catalysis without loss in Faradaic efficiency (Figure 7b, Table 1). By voltammetry, catalysis by **5** reaches 2.25 mA at −0.80 V vs SHE ( $\eta$  = 390 mV), whereas the unsubstituted parent complex **4** requires −0.97 V vs SHE ( $\eta$  = 560 mV). Introduction of an electron-donating dimethylamino substituent (**6**, Figure 2) increases the requisite driving force by another 100 mV. Independent preparation of the Co(I) complex [(PYSMe<sub>2</sub>)Co]<sup>+</sup> reveals that it shares its square pyramidal coordination geometry and its intense blue coloration with the cobaloxime anions,<sup>37–40</sup> but instead it possesses a high-spin d<sup>8</sup> electron configuration. In addition, we established that **5** can generate hydrogen from neutral water under photocatalytic conditions with visible light irradiation, [Ru(bpy)<sub>3</sub>]<sup>2+</sup> as a molecular photosensitizer, and ascorbic acid as a sacrificial reductant (Figure 8).<sup>41</sup> Likewise, **5** enhanced the hydrogen photolysis yield of GaP nanowires in water, demonstrating that this molecular catalyst platform can be interfaced with heterogeneous photosensitizers.<sup>41</sup> Taken together, these results suggest that judicious modifications of the ancillary ligand can furnish catalysts active in water, utilizing either sustainable solar or electrical input.

## ■ REDOX-ACTIVE LIGANDS FOR REDOX-LEVELING AND FACILITATING MULTIELECTRON ELECTROCATALYSIS

The prevalence of molecular cobalt-based proton reduction catalysts,<sup>9,39,40,42–63</sup> including contributions from our

**Table 2.** Photolytic Hydrogen Production by Molecular Cobalt Catalysts<sup>a</sup>

	TON (mol H <sub>2</sub> (mol cat) <sup>−1</sup> )	TOF (mol H <sub>2</sub> (mol cat h) <sup>−1</sup> )	pH with highest activity	reaction time (h)	ref
1	1015	73	4.5	14	65
4	290	22	6.0	13	64
5	300	23	6.0	13	64
7	1625	125	4.0	13	64
8	1375	106	4.5	13	64
9	1875	134	4.0	14	65
10	425	30	4.5	14	65
11	1065	76	4.0	14	65
12	235	13	5.0	18	65
13	260	14	5.5	18	65
14	1565	87	5.0	18	65
15	225	16	5.5	14	65
16	150	11	5.0	14	65

<sup>a</sup>Photolysis conditions: 330 μM [Ru(bpy)<sub>3</sub>]<sup>2+</sup>, 0.3 M ascorbate buffer, and 20 μM catalyst in water, irradiated at 452 nm with 540 mW output.

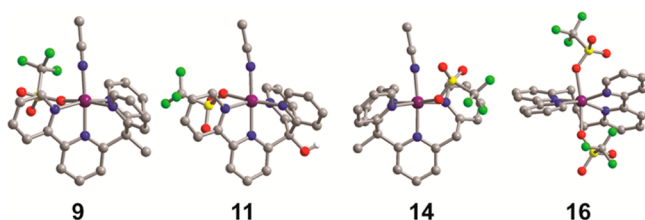


**Figure 10.** Crystal structures of **9**, **11**, **14**, and **16**;  $R_1$  ( $wR_2$ ) = 2.53% (6.58%), 2.75% (11.3%), 2.77% (6.60%), and 2.96% (7.01%), respectively. **9**, **11**, and **14** contain two *cis* open sites, whereas **16** has two *trans* open sites.

laboratories,<sup>11,16,36,37,41,64,65</sup> has attracted many experimental and computational mechanistic investigations. Although the operative mechanism for these catalysts can vary widely, formation of a cobalt-hydride is commonly invoked.<sup>37,48</sup> With interest in minimizing catalyst overpotentials, Co(I) centers capable of deprotonating water (or  $H^+$ <sub>(aq)</sub>) are more desirable than resorting to the undoubtedly more basic Co(0) species, which require an additional reducing equivalent and thus more negative potentials (Figure 9a). In cases where protonation of Co(I) is inefficient, however, we reasoned that introduction of another ligand-based redox event between the Co(II/I) and

Co(I/0) couples may lower catalyst overpotentials. This concept is challenging to put into practice, however, as incorporation of a redox-active ligand can have detrimental effects. For example, the delocalization of spin onto the ligand framework in Co-bisglyoxime<sup>39,40,42</sup> and trisglyoxime<sup>66</sup> catalysts have been shown to promote ligand hydrogenation<sup>67–70</sup> during catalysis, significantly reducing catalyst longevity.

We therefore designed the complex [(bpy2PYMe)Co(CF<sub>3</sub>SO<sub>3</sub>)<sup>1+</sup>] (7, Figure 2),<sup>64</sup> which contains two 2,2'-bipyridine (bpy) moieties that are not only redox-active but also expected to be robust against hydrogenation, vis-à-vis oximes, owing to their aromatic nature (Figure 9b). Indeed, the CV of 7 in acetonitrile displays a metal-centered Co(II/I) couple followed by two  $bpy^{0/+}$  reductions. Addition of acetic acid, which possesses a  $H^+/H_2$  reduction potential midway of the Co(II/I) and  $bpy^{0/+}$  couples, engenders electrocatalysis. Complex 7 can also reduce water photocatalytically under fully aqueous conditions with [Ru(bpy)<sub>3</sub>]<sup>2+</sup> and ascorbic acid. Although the catalyst is not indefinitely stable under irradiation, this photocatalytic system is apparently limited by the durability of the photosensitizer. Addition of [Ru(bpy)<sub>3</sub>]<sup>2+</sup> after catalysis levels off restores activity (Figure 9c), whereas addition of fresh

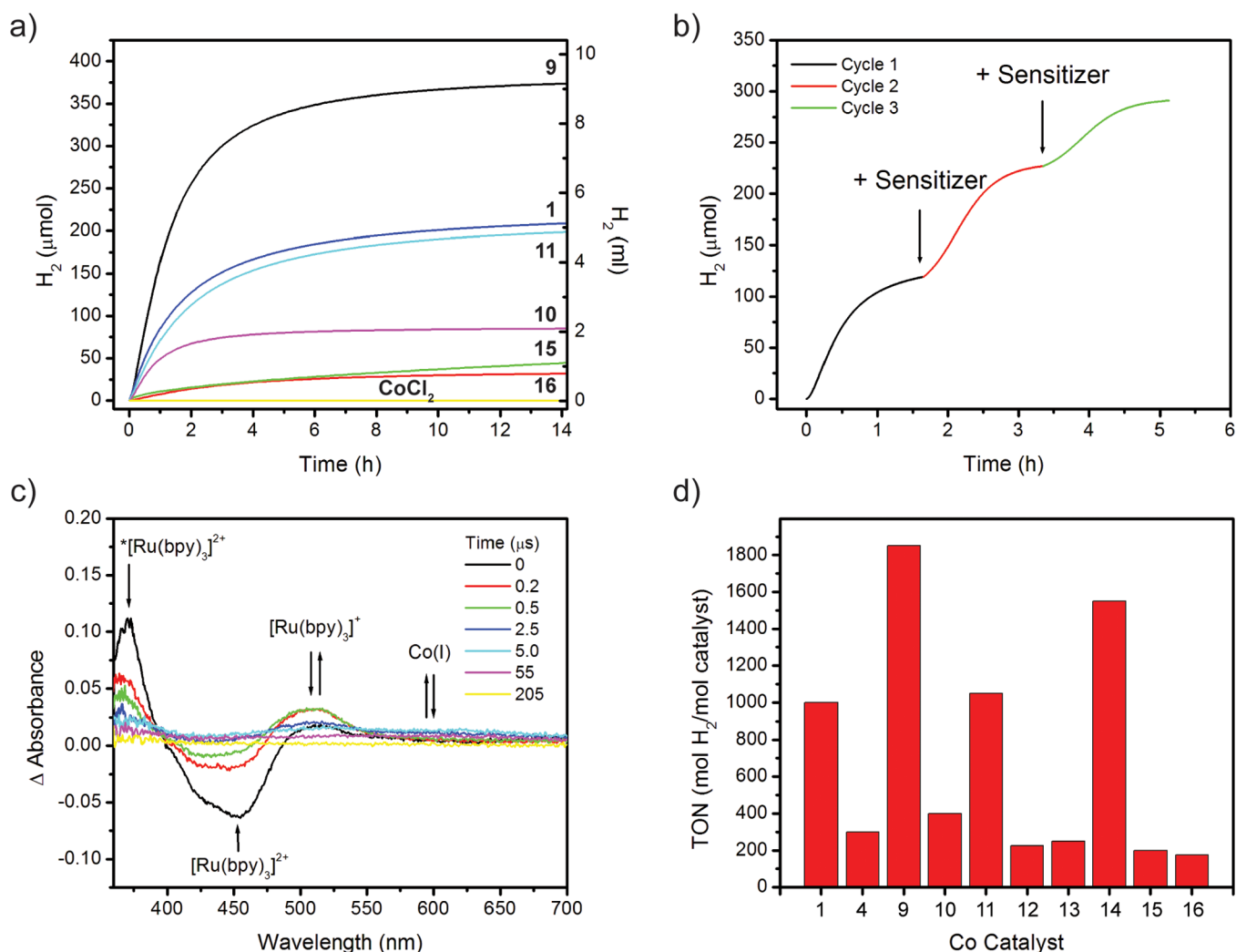


**Figure 11.** (a) Photocatalytic hydrogen production versus time of different Co catalysts. (b) Catalysis is limited by photosensitizer stability. (c) Transient absorption difference spectra shows formation of a Co(I) species of **9** coinciding with disappearance of [Ru(bpy)<sub>3</sub>]<sup>2+</sup>. (d) TONs of different Co catalysts at their respective optimal pH.



catalyst in parallel experiments did not. Photocatalysis by **4** and **5**, which are devoid of redox-active ligands, result in ca. 6-fold decrease in activity relative to that by **7** (Table 2), showcasing synergy between ligand and metal redox activity.

## ■ OPTIMIZING PHOTOCATALYTIC HYDROGEN GENERATION

The foregoing results prompted us to evaluate the photocatalytic performance of other cobalt(II)-based molecular catalysts. Importantly, these experiments required catalyst concentrations only at the micromolar level, enabling us to interrogate complexes that were not soluble enough for conventional aqueous electrochemistry. Again, using  $[\text{Ru}(\text{bpy})_3]^{2+}$  and an aqueous ascorbate buffer, we evaluated the photocatalytic properties of 10 cobalt–polypyridyl catalysts, including **9**, **11**, **14**, and **16** (Figure 10), using a high-throughput photochemical reactor developed by Castellano.<sup>65</sup> These findings highlighted several trends. First, Co(II) complexes bearing tetradentate ligands that enforce *cis* divacant coordination sites, such as **1**, **9**, **10**, and **11**, show higher activity for photocatalytic hydrogen generation compared those with ligands that enforce *trans* sites, **15** and **16** (Figure 11a). Second, sustained photochemical hydrogen production is limited by the stability of  $[\text{Ru}(\text{bpy})_3]^{2+}$ , not the catalyst (Figure 11b). Third, transient absorption measurements suggest that a putative Co(I) intermediate forms during photocatalysis (Figure 11c). Finally, changes in pH had different effects on the activity for each catalyst. With each catalyst evaluated at its optimal pH, comparison of TONs reveal that catalysts with tetradentate ligands exhibit higher activity than that of those bearing pentadentate ligands, without losses in stability (Figure 11d, Table 2). The performance of **14**, which does not contain redox-active ligands, exemplifies the importance of denticity and implies that the operative photocatalytic mechanism in water substantially differs from the electrochemical mechanism utilizing weak organic acids.

## ■ CONCLUDING REMARKS

In this Account, we have summarized recent progress in our laboratories in the creation of molecular catalysts for electrochemical and photochemical water reduction. Specifically, we have developed a family of molybdenum– and cobalt–polypyridyl proton reduction catalysts that operate in pure water with high, selective, and robust activity. The foregoing examples highlight how molecular systems can conceptually and practically shed large portions of enzymatic and heterogeneous catalysts while retaining the minimal chemical unit needed for catalytic function. As such, molecular systems provide a useful, complementary approach to biological and materials catalysts for sustainable solar-to-fuel conversion. This work sets the stage for the broader application of polypyridyl systems to catalysis under environmentally benign aqueous conditions.

## ■ AUTHOR INFORMATION

### Corresponding Authors

\*(J.R.L.) E-mail: jrlong@berkeley.edu.

\*(C.J.C.) E-mail: chrischang@berkeley.edu.

### Author Contributions

<sup>∇</sup>D.Z.Z. and T.C. contributed equally to this work.

### Notes

The authors declare no competing financial interest.

## Biographies

**David Z. Zee** received a B.A. degree in Chemistry and Economics from Swarthmore College in 2007. He joined the laboratory of Prof. Jeffrey Long at UC Berkeley and was awarded a NSF Graduate Research Fellowship. His research interests lie in water and CO<sub>2</sub> reduction catalysis and the activation of other small molecule substrates relevant for sustainable energy purposes.

**Teera Chantarojsiri** was awarded a Development and Promotion of Science and Technology scholarship (DPST) from the Thai government in 2005 to study Chemistry. She received her B.S. (honors) in Chemistry from Stanford University in 2010, where she conducted research under the supervision of Prof. Dan Stack. She is currently completing her Ph.D. at UC Berkeley in the laboratory of Prof. Christopher Chang working on inorganic synthesis and small molecule activations.

**Jeffrey R. Long** received a B.A. degree from Cornell University in 1991 and earned his Ph.D. from Harvard University in 1995. Following postdoctoral work at Harvard and the University of California, Berkeley, he joined the faculty at Berkeley in 1997, where he is currently Professor of Chemistry. He is also a Senior Faculty Scientist in the Materials Sciences Division of Lawrence Berkeley National Laboratory. In addition, he is the lead-PI for the Berkeley Hydrogen Storage Program, Director of the Center for Gas Separations, and a cofounder of Mosaic Materials, Inc. His research areas include the synthesis of inorganic clusters and solids with unusual electronic and magnetic properties, generation of microporous metal–organic frameworks for applications in gas storage, separations, and catalysis, and the development of molecular catalysts for electro- and photochemical water splitting.

**Christopher J. Chang** is the Class of 1942 Chair Professor in the Departments of Chemistry and Molecular and Cell Biology at UC Berkeley, Howard Hughes Medical Institute Investigator, and Faculty Scientist in the Chemical Sciences Division of Lawrence Berkeley National Laboratory. He is a Senior Editor of ACS Central Science. Chris received his B.S. and M.S. degrees from Caltech in 1997, studied as a Fulbright scholar in Strasbourg, France, and received his Ph.D. from MIT in 2002 with Dan Nocera. After postdoctoral studies with Steve Lippard, Chris joined the UC Berkeley faculty in 2004. Research in the Chang lab is focused on chemical biology and inorganic chemistry, with particular interests in molecular imaging and catalysis applied to neuroscience and sustainable energy. His group's work has been honored by awards from the Dreyfus, Beckman, Sloan, and Packard Foundations, Amgen, AstraZeneca, and Novartis, Technology Review, ACS (Cope Scholar, Eli Lilly, Nobel Laureate Signature, Baekeland), RSC (Transition Metal Chemistry), and SBIC.

## ■ ACKNOWLEDGMENTS

Our work in sustainable energy catalysis is funded by DOE/LBNL Grant 101528-002 (T.C. and C.J.C.) and the Joint Center for Artificial Photosynthesis, a DOE Energy Innovation Hub, supported through the Office of Science of the U.S. Department of Energy award DE-SC0004993 (D.Z.Z. and J.R.L.). T.C. is supported by a DPST scholarship from the Thai government. D.Z.Z. thanks the National Science Foundation for a Graduate Research Fellowship. C.J.C. is an Investigator with the Howard Hughes Medical Institute.

## ■ REFERENCES

(1) Bard, A. J.; Fox, M. A. Artificial Photosynthesis: Solar Splitting of Water to Hydrogen and Oxygen. *Acc. Chem. Res.* **1995**, *28*, 141–145.



- (2) Turner, J. A. Sustainable Hydrogen Production. *Science* **2004**, *305*, 972–974.
- (3) Gordon, R. B.; Bertram, M.; Graedel, T. E. Metal Stocks and Sustainability. *Proc. Natl. Acad. Sci. U.S.A.* **2006**, *103*, 1209–1214.
- (4) Lewis, N. S.; Nocera, D. G. Powering the Planet: Chemical Challenges in Solar Energy Utilization. *Proc. Natl. Acad. Sci. U.S.A.* **2006**, *103*, 15729–15735.
- (5) Armstrong, F. Hydrogenases: Active Site Puzzles and Progress. *Curr. Opin. Chem. Biol.* **2004**, *8*, 133–140.
- (6) Fontecilla-Camps, J. C.; Volbeda, A.; Cavazza, C.; Nicolet, Y. Structure/Function Relationships of [NiFe]- and [FeFe]-Hydrogenases. *Chem. Rev.* **2007**, *107*, 4273–4303.
- (7) Barton, B. E.; Olsen, M. T.; Rauchfuss, T. B. Artificial Hydrogenases. *Curr. Opin. Biotechnol.* **2010**, *21*, 292–297.
- (8) Cook, T. R.; Dogutan, D. K.; Reece, S. Y.; Surendranath, Y.; Teets, T. S.; Nocera, D. G. Solar Energy Supply and Storage for the Legacy and Nonlegacy Worlds. *Chem. Rev.* **2010**, *110*, 6474–6502.
- (9) Artero, V.; Chavarot-Kerlidou, M.; Fontecave, M. Splitting Water with Cobalt. *Angew. Chem., Int. Ed.* **2011**, *50*, 7238–7266.
- (10) Wang, M.; Chen, L.; Sun, L. Recent Progress in Electrochemical Hydrogen Production with Earth-Abundant Metal Complexes as Catalysts. *Energy Environ. Sci.* **2012**, *5*, 6763–6778.
- (11) Thoi, V. S.; Sun, Y.; Long, J. R.; Chang, C. J. Complexes of Earth-Abundant Metals for Catalytic Electrochemical Hydrogen Generation under Aqueous Conditions. *Chem. Soc. Rev.* **2013**, *42*, 2388–2400.
- (12) McKone, J. R.; Marinescu, S. C.; Brunschwig, B. S.; Winkler, J. R.; Gray, H. B. Earth-Abundant Hydrogen Evolution Electrocatalysts. *Chem. Sci.* **2014**, *5*, 865–878.
- (13) Bullock, R. M.; Appel, A. M.; Helm, M. L. Production of Hydrogen by Electrocatalysis: Making the H–H Bond by Combining Protons and Hydrides. *Chem. Commun.* **2014**, *50*, 3125–3143.
- (14) Han, Z.; Eisenberg, R. Fuel From Water: the Photochemical Generation of Hydrogen From Water. *Acc. Chem. Res.* **2014**, *47*, 2537–2544.
- (15) DuBois, D. L. Development of Molecular Electrocatalysts for Energy Storage. *Inorg. Chem.* **2014**, *53*, 3935–3960.
- (16) Bigi, J. P.; Hanna, T. E.; Harman, W. H.; Chang, A.; Chang, C. J. Electrocatalytic Reduction of Protons to Hydrogen by a Water-Compatible Cobalt Polypyridyl Platform. *Chem. Commun.* **2010**, *46*, 958–960.
- (17) Goldsmith, C. R.; Jonas, R. T.; Stack, T. D. P. C–H Bond Activation by a Ferric Methoxide Complex: Modeling the Rate-Determining Step in the Mechanism of Lipoyxygenase. *J. Am. Chem. Soc.* **2002**, *124*, 83–96.
- (18) Klein Gebbink, R. J. M.; Jonas, R. T.; Goldsmith, C. R.; Stack, T. D. P. A Periodic Walk: A Series of First-Row Transition Metal Complexes with the Pentadentate Ligand PY5. *Inorg. Chem.* **2002**, *41*, 4633–4641.
- (19) Goldsmith, C. R.; Jonas, R. T.; Cole, A. P.; Stack, T. D. P. A Spectrochemical Walk: Single-Site Perturbation within a Series of Six-Coordinate Ferrous Complexes. *Inorg. Chem.* **2002**, *41*, 4642–4652.
- (20) Bechlars, B.; D'Alessandro, D. M.; Jenkins, D. M.; Iavarone, A. T.; Glover, S. D.; Kubiak, C. P.; Long, J. R. High-Spin Ground States via Electron Delocalization in Mixed-Valence Imidazolate-Bridged Divanadium Complexes. *Nat. Chem.* **2010**, *2*, 362–368.
- (21) Parkin, G.; Bercaw, J. E. ( $\eta^5$ -C<sub>5</sub>Me<sub>5</sub>)<sub>2</sub>W=O: An Exceptionally Reactive Organometallic Oxo Derivative. Reduction with Dihydrogen and Reaction with Dioxygen Resulting in Insertion of Oxygen into a Tungsten–Carbon Bond. *J. Am. Chem. Soc.* **1989**, *111*, 391–393.
- (22) Silavwe, N. D.; Bruce, M. R. M.; Philbin, C. E.; Tyler, D. R. Descriptive Photochemistry and Electronic Structure of the Cp<sub>2</sub>MoO and (MeCp)<sub>2</sub>MoO Complexes (Cp =  $\eta^5$ -C<sub>5</sub>H<sub>5</sub>; MeCp =  $\eta^5$ -CH<sub>3</sub>C<sub>5</sub>H<sub>4</sub>). *Inorg. Chem.* **1988**, *27*, 4669–4676.
- (23) Yoon, M.; Tyler, D. R. Activation of Water by Permethyltungstenocene; Evidence for the Oxidative Addition of Water. *Chem. Commun.* **1997**, 639–670.
- (24) Baxley, G. T.; Avey, A. A.; Aukett, T. M.; Tyler, D. R. Photoactivation of Water by Cp<sub>2</sub>Mo and Photochemical Studies of Cp<sub>2</sub>MoO. Investigation of a Proposed Water-Splitting Cycle and Preparation of a Water-Soluble Molybdocene Dihydride. *Inorg. Chim. Acta* **2000**, *300*, 102–112.
- (25) Blum, O.; Milstein, D. Oxidative Addition of Water and Aliphatic Alcohols by IrCl(trialkylphosphine)<sub>3</sub>. *J. Am. Chem. Soc.* **2002**, *124*, 11456–11467.
- (26) Karunadasa, H. I.; Chang, C. J.; Long, J. R. A Molecular Molybdenum-Oxo Catalyst for Generating Hydrogen from Water. *Nature* **2010**, *464*, 1329–1333.
- (27) Thoi, V. S.; Karunadasa, H. I.; Surendranath, Y.; Long, J. R.; Chang, C. J. Electrochemical Generation of Hydrogen from Acetic Acid Using a Molecular Molybdenum–Oxo Catalyst. *Energy Environ. Sci.* **2012**, *5*, 7762–7770.
- (28) Sundstrom, E. J.; Yang, X.; Thoi, V. S.; Karunadasa, H. I.; Chang, C. J.; Long, J. R.; Head-Gordon, M. Computational and Experimental Study of the Mechanism of Hydrogen Generation from Water by a Molecular Molybdenum–Oxo Electrocatalyst. *J. Am. Chem. Soc.* **2012**, *134*, 5233–5242.
- (29) Hinnemann, B.; Moses, P. G.; Bonde, J.; Jørgensen, K. P.; Nielsen, J. H.; Horch, S.; Chorkendorff, I.; Nørskov, J. K. Biomimetic Hydrogen Evolution: MoS<sub>2</sub> Nanoparticles as Catalyst for Hydrogen Evolution. *J. Am. Chem. Soc.* **2005**, *127*, 5308–5309.
- (30) Jaramillo, T. F.; Jørgensen, K. P.; Bonde, J.; Nielsen, J. H.; Horch, S.; Chorkendorff, I. Identification of Active Edge Sites for Electrochemical H<sub>2</sub> Evolution from MoS<sub>2</sub> Nanocatalysts. *Science* **2007**, *317*, 100–102.
- (31) Zong, X.; Yan, H.; Wu, G.; Ma, G.; Wen, F.; Wang, L.; Li, C. Enhancement of Photocatalytic H<sub>2</sub> Evolution on CdS by Loading MoS<sub>2</sub> as Cocatalyst under Visible Light Irradiation. *J. Am. Chem. Soc.* **2008**, *130*, 7176–7177.
- (32) Li, Y.; Wang, H.; Xie, L.; Liang, Y.; Hong, G.; Dai, H. MoS<sub>2</sub> Nanoparticles Grown on Graphene: An Advanced Catalyst for the Hydrogen Evolution Reaction. *J. Am. Chem. Soc.* **2011**, *133*, 7296–7299.
- (33) Merki, D.; Fierro, S.; Vrubel, H.; Hu, X. Amorphous Molybdenum Sulfide Films as Catalysts for Electrochemical Hydrogen Production in Water. *Chem. Sci.* **2011**, *2*, 1262–1267.
- (34) Lukowski, M. A.; Daniel, A. S.; Meng, F.; Forticaux, A.; Li, L.; Jin, S. Enhanced Hydrogen Evolution Catalysis from Chemically Exfoliated Metallic MoS<sub>2</sub> Nanosheets. *J. Am. Chem. Soc.* **2013**, *135*, 10274–10277.
- (35) Karunadasa, H. I.; Montalvo, E.; Sun, Y.; Majda, M.; Long, J. R.; Chang, C. J. A Molecular MoS<sub>2</sub> Edge Site Mimic for Catalytic Hydrogen Generation. *Science* **2012**, *335*, 698–702.
- (36) Sun, Y.; Bigi, J. P.; Piro, N. A.; Tang, M. L.; Long, J. R.; Chang, C. J. Molecular Cobalt Pentapyridine Catalysts for Generating Hydrogen from Water. *J. Am. Chem. Soc.* **2011**, *133*, 9212–9215.
- (37) King, A. E.; Surendranath, Y.; Piro, N. A.; Bigi, J. P.; Long, J. R.; Chang, C. J. A Mechanistic Study of Proton Reduction Catalyzed by a Pentapyridine Cobalt Complex: Evidence for Involvement of an Anation-Based Pathway. *Chem. Sci.* **2013**, *4*, 1578–1587.
- (38) Shi, S.; Daniels, L. M.; Espenson, J. H. Molecular Structure of a Cobalt(I) Complex Lacking a Carbonyl Ligand. A Unique Example of Cobalt–Nitrogen Bond Shortening. *Inorg. Chem.* **1991**, *30*, 3407–3410.
- (39) Hu, X.; Cossairt, B. M.; Brunschwig, B. S.; Lewis, N. S.; Peters, J. C. Electrocatalytic Hydrogen Evolution by Cobalt Difluoroboryl–Diglyoximate Complexes. *Chem. Commun.* **2005**, 4723–4725.
- (40) Hu, X.; Brunschwig, B. S.; Peters, J. C. Electrocatalytic Hydrogen Evolution at Low Overpotentials by Cobalt Macrocyclic Glyoxime and Tetraimine Complexes. *J. Am. Chem. Soc.* **2007**, *129*, 8988–8998.
- (41) Sun, Y.; Sun, J.; Long, J. R.; Yang, P.; Chang, C. J. Photocatalytic Generation of Hydrogen From Water Using a Cobalt Pentapyridine Complex in Combination with Molecular and Semiconductor Nanowire Photosensitizers. *Chem. Sci.* **2013**, *4*, 118–124.
- (42) Razavet, M.; Artero, V.; Fontecave, M. Proton Electroreduction Catalyzed by Cobaloximes: Functional Models for Hydrogenases. *Inorg. Chem.* **2005**, *44*, 4786–4795.

- (43) Baffert, C.; Artero, V.; Fontecave, M. Cobaloximes as Functional Models for Hydrogenases. 2. Proton Electoreduction Catalyzed by Difluoroborylbis(dimethylglyoximate)cobalt(II) Complexes in Organic Media. *Inorg. Chem.* **2007**, *46*, 1817–1824.
- (44) Fourmond, V.; Jacques, P.-A.; Fontecave, M.; Artero, V. H<sub>2</sub> Evolution and Molecular Electrocatalysts: Determination of Overpotentials and Effect of Homoconjugation. *Inorg. Chem.* **2010**, *49*, 10338–10347.
- (45) McCrory, C. C. L.; Uyeda, C.; Peters, J. C. Electrocatalytic Hydrogen Evolution in Acidic Water with Molecular Cobalt Tetraazamacrocycles. *J. Am. Chem. Soc.* **2012**, *134*, 3164–3170.
- (46) Jacobsen, G. M.; Yang, J. Y.; Twamley, B.; Wilson, A. D.; Bullock, R. M.; Rakowski DuBois, M.; DuBois, D. L. Hydrogen Production Using Cobalt-Based Molecular Catalysts Containing a Proton Relay in the Second Coordination Sphere. *Energy Environ. Sci.* **2008**, *1*, 167–174.
- (47) Fang, M.; Wiedner, E. S.; Dougherty, W. G.; Kassel, W. S.; Liu, T.; DuBois, D. L.; Bullock, R. M. Cobalt Complexes Containing Pendant Amines in the Second Coordination Sphere as Electrocatalysts for H<sub>2</sub> Production. *Organometallics* **2014**, *33*, 5820–5833.
- (48) Dempsey, J. L.; Brunschwig, B. S.; Winkler, J. R.; Gray, H. B. Hydrogen Evolution Catalyzed by Cobaloximes. *Acc. Chem. Res.* **2009**, *42*, 1995–2004.
- (49) Dempsey, J. L.; Winkler, J. R.; Gray, H. B. Kinetics of Electron Transfer Reactions of H<sub>2</sub>-Evolving Cobalt Diglyoxime Catalysts. *J. Am. Chem. Soc.* **2010**, *132*, 1060–1065.
- (50) Stubbert, B. D.; Peters, J. C.; Gray, H. B. Rapid Water Reduction to H<sub>2</sub> Catalyzed by a Cobalt Bis(iminopyridine) Complex. *J. Am. Chem. Soc.* **2011**, *133*, 18070–18073.
- (51) Marinescu, S. C.; Winkler, J. R.; Gray, H. B. Molecular Mechanisms of Cobalt-Catalyzed Hydrogen Evolution. *Proc. Natl. Acad. Sci. U.S.A.* **2012**, *109*, 15127–15131.
- (52) McNamara, W. R.; Han, Z.; Alperin, P. J.; Brennessel, W. W.; Holland, P. L.; Eisenberg, R. A Cobalt–Dithiolene Complex for the Photocatalytic and Electrocatalytic Reduction of Protons. *J. Am. Chem. Soc.* **2011**, *133*, 15368–15371.
- (53) McNamara, W. R.; Han, Z.; Yin, C.-J. M.; Brennessel, W. W.; Holland, P. L.; Eisenberg, R. Cobalt–Dithiolene Complexes for the Photocatalytic and Electrocatalytic Reduction of Protons in Aqueous Solutions. *Proc. Natl. Acad. Sci. U.S.A.* **2012**, *109*, 15594–15599.
- (54) Probst, B.; Guttentag, M.; Rodenberg, A.; Hamm, P.; Alberto, R. Photocatalytic H<sub>2</sub> Production from Water with Rhenium and Cobalt Complexes. *Inorg. Chem.* **2011**, *50*, 3404–3412.
- (55) Rodenberg, A.; Oraziotti, M.; Probst, B.; Bachmann, C.; Alberto, R.; Baldrige, K. K.; Hamm, P. Mechanism of Photocatalytic Hydrogen Generation by a Polypyridyl-Based Cobalt Catalyst in Aqueous Solution. *Inorg. Chem.* **2015**, *54*, 646–657.
- (56) Chen, L.; Wang, M.; Han, K.; Zhang, P.; Gloaguen, F.; Sun, L. A Super-Efficient Cobalt Catalyst for Electrochemical Hydrogen Production from Neutral Water with 80 mV Overpotential. *Energy Environ. Sci.* **2013**, *7*, 329–334.
- (57) Zhang, P.; Wang, M.; Gloaguen, F.; Chen, L.; Quentel, F.; Sun, L. Electrocatalytic Hydrogen Evolution from Neutral Water by Molecular Cobalt Tripyridine–Diamine Complexes. *Chem. Commun.* **2013**, *49*, 9455–9457.
- (58) Singh, W. M.; Baine, T.; Kudo, S.; Tian, S.; Ma, X. A. N.; Zhou, H.; DeYonker, N. J.; Pham, T. C.; Bollinger, J. C.; Baker, D. L.; Yan, B.; Webster, C. E.; Zhao, X. Electrocatalytic and Photocatalytic Hydrogen Production in Aqueous Solution by a Molecular Cobalt Complex. *Angew. Chem., Int. Ed.* **2012**, *51*, 5941–5944.
- (59) Lee, C. H.; Dogutan, D. K.; Nocera, D. G. Hydrogen Generation by Hangman Metalloporphyrins. *J. Am. Chem. Soc.* **2011**, *133*, 8775–8777.
- (60) Singh, W. M.; Mirmohades, M.; Jane, R. T.; White, T. A.; Hammarström, L.; Thapper, A.; Lomoth, R.; Ott, S. Voltammetric and Spectroscopic Characterization of Early Intermediates in the Co(II)–Polypyridyl-Catalyzed Reduction of Water. *Chem. Commun.* **2013**, *49*, 8638–8640.
- (61) Mandal, S.; Shikano, S.; Yamada, Y.; Lee, Y.-M.; Nam, W.; Llobet, A.; Fukuzumi, S. Protonation Equilibrium and Hydrogen Production by a Dinuclear Cobalt–Hydride Complex Reduced by Cobaltocene with Trifluoroacetic Acid. *J. Am. Chem. Soc.* **2013**, *135*, 15294–15297.
- (62) Tong, L.; Zong, R.; Thummel, R. P. Visible Light-Driven Hydrogen Evolution from Water Catalyzed by a Molecular Cobalt Complex. *J. Am. Chem. Soc.* **2014**, *136*, 4881–4884.
- (63) Letko, C. S.; Panetier, J. A.; Head-Gordon, M.; Tilley, T. D. Mechanism of the Electrocatalytic Reduction of Protons with Diaryldithiolene Cobalt Complexes. *J. Am. Chem. Soc.* **2014**, *136*, 9364–9376.
- (64) Nippe, M.; Khnayzer, R. S.; Panetier, J. A.; Zee, D. Z.; Olaiya, B. S.; Head-Gordon, M.; Chang, C. J.; Castellano, F. N.; Long, J. R. Catalytic Proton Reduction with Transition Metal Complexes of the Redox-Active Ligand bpy2PYMe. *Chem. Sci.* **2013**, *4*, 3934–3945.
- (65) Khnayzer, R. S.; Thoi, V. S.; Nippe, M.; King, A. E.; Jurs, J. W.; Roz, E. K. A.; Long, J. R.; Chang, C. J.; Castellano, F. N. Towards a Comprehensive Understanding of Visible-Light Photogeneration of Hydrogen from Water Using Cobalt(II) Polypyridyl Catalysts. *Energy Environ. Sci.* **2014**, *7*, 1477–1488.
- (66) Voloshin, Y. Z.; Dolganov, A. V.; Varzatskii, O. A.; Bubnov, Y. N. Efficient Electrocatalytic Hydrogen Production from H<sup>+</sup> Ions Using Specially Designed Boron-Capped Cobalt Clathrochelates. *Chem. Commun.* **2011**, *47*, 7737–7739.
- (67) Anxolabéhère-Mallart, E.; Costentin, C.; Fournier, M.; Nowak, S.; Robert, M.; Savéant, J.-M. Boron-Capped Tris(glyoximate) Cobalt Clathrochelate as a Precursor for the Electrodeposition of Nanoparticles Catalyzing H<sub>2</sub> Evolution in Water. *J. Am. Chem. Soc.* **2012**, *134*, 6104–6107.
- (68) El Ghachtouli, S.; Fournier, M.; Cherdo, S.; Guillot, R.; Charlot, M.-F.; Anxolabéhère-Mallart, E.; Robert, M.; Aukaaloo, A. Monometallic Cobalt–Trisglyoximate Complexes as Precatalysts for Catalytic H<sub>2</sub> Evolution in Water. *J. Phys. Chem. C* **2013**, *117*, 17073–17077.
- (69) El Ghachtouli, S.; Guillot, R.; Brisset, F.; Aukaaloo, A. Cobalt-Based Particles Formed upon Electrocatalytic Hydrogen Production by a Cobalt Pyridine Oxime Complex. *ChemSusChem* **2013**, *6*, 2226–2230.
- (70) Anxolabéhère-Mallart, E.; Costentin, C.; Fournier, M.; Robert, M. Cobalt–Bisglyoximate Diphenyl Complex as a Precatalyst for Electrocatalytic H<sub>2</sub> Evolution. *J. Phys. Chem. C* **2014**, *118*, 13377–13381.
- (71) Artero, V.; Savéant, J.-M. Toward the Rational Benchmarking of Homogeneous H<sub>2</sub>-Evolving Catalysts. *Energy Environ. Sci.* **2014**, *7*, 3808–3814.